JOURNAL OF GUIDANCE, CONTROL, AND DYNAMICS
Vol. 30, No. 4, July–August 2007

Orbital Rendezvous and Flyaround Based on Null Controllability with Vanishing Energy

Motoyuki Shibata* and Akira Ichikawa†
Kyoto University, Kyoto 606-8501, Japan

DOI: 10.2514/1.24171

Hill's equations describe the relative motion of a chaser with respect to the target spacecraft in a circular orbit. They possess periodic solutions that form the relative orbits of the chaser. In this paper it is shown that Hill's equations with three independent control accelerations are null controllable with vanishing energy. Based on this property, the relative orbit transfer problem is formulated as a linear quadratic regulator problem and a feedback control with arbitrary small L^2 norm is obtained via the Riccati equation. The design method is then extended to Tschauner–Hempel equations that describe the relative motion of the chaser along an eccentric orbit. It is shown that the controlled Tschauner–Hempel equations are also null controllable with vanishing energy and a feedback control with arbitrary small L^2 norm is designed using the periodic solution of the Riccati differential equation. Numerical simulations of Hill's equations as well as Tschauner–Hempel equations are given and feedback controls with good performance are obtained.

Nomenclature

A	=	state matrix
a	=	semiminor axis of relative elliptic orbit
B	=	control matrix
d	=	y coordinate of center of ellipse
e	=	eccentricity of ellipse
G	=	universal gravitational constant
h_c	=	height of circular orbit
h_p, h_a	=	height at perigee and apogee of eccentric orbit
$J(\boldsymbol{u}, \boldsymbol{x}_0)$	=	quadratic cost
$\hat{J}$	=	minimum cost
K	=	parameter of relative orbit along eccentric orbit
n	=	orbit rate
P	=	matrix of minimum cost in parameter space
Q	=	penalty matrix on state
R	=	penalty matrix on control
R_0	=	distance between target spacecraft and Earth
$S(t, s)$	=	state transition matrix
T	=	period of orbit
T_s	=	settling time
$\boldsymbol{u}$	=	input vector
X	=	solution of algebraic Riccati equation
$\boldsymbol{x}$	=	state vector
(x, y, z)	=	rotating coordinate frame fixed in target spacecraft
ΔV_T	=	total velocity change of two-impulse maneuver
ϵ_r	=	parameter of stopping rule
θ	=	true anomaly
μ_e	=	gravitational parameter of Earth
(ξ, η)	=	parameters of initial condition of tracking error
τ	=	time parameter of initial condition
Φ_θ	=	fundamental matrix
$\dot{\cdot}$	=	derivative of $\cdot$ with respect to time

Received 24 March 2006; revision received 25 February 2007; accepted for publication 8 March 2007.

*Graduate Student, Department of Aeronautics and Astronautics; currently Engineer, Vehicle Engineering Group, Toyota Motor Corporation, Toyota 471-8571, Japan.

†Professor, Department of Aeronautics and Astronautics; ichikawa@kuaero.kyoto-u.ac.jp.

I. Introduction

CONSIDER a spacecraft in a circular orbit and another in its vicinity, which are referred to as the target and the chaser, respectively. The relative motion of the chaser with respect to the target is described by autonomous nonlinear differential equations. The linearized equations are known as Hill's equations or Clohessy–Wiltshire equations [1–4]. They are used in many research works concerning rendezvous [5–8] and formation flight [9–17]. Hill's equations possess periodic solutions and the trajectories of the in-plane motion form ellipses. These solutions constitute relative orbits of the chaser and are useful for passive rendezvous and formation flight because no energy is required for the chaser to stay in a relative orbit. Such orbits could be used as temporary orbits before mission. Relative orbits of a small size would be convenient for proximity operations such as inspection and repair. For long-term space missions a series of operations are generally planned, and relative orbit transfers are needed when the operation of a spacecraft changes. Therefore it is useful to consider the relative orbit transfer problem and to develop a good control strategy for the transfer.

When the target is in an eccentric orbit, the relative motion of the chaser is described by nonlinear differential equations with periodic coefficients. The linearized equations are known as the Tschauner–Hempel equations [7,18]. The state transition matrix associated with them is given in various forms [7,19]. The Tschauner–Hempel equations also possess periodic solutions that constitute relative orbits and are used for the study of rendezvous and formation flight [18,20].

For rendezvous problems, fixed-time and fixed-end conditions are often assumed and impulsive maneuvers are employed [5,6,18]. For formation flying, impulsive maneuvers are also used [14], but various approaches such as linear quadratic regulator (LQR) [11–13], adaptive control [15], and nonlinear control [16] are employed.

In this paper the relative orbit transfer problems associated with Hill's equations and the Tschauner–Hempel equations are considered and a design method of feedback controllers that require less energy is proposed. For this purpose three independent continuous control accelerations (or thrusts) are introduced to both Hill's equations and Tschauner–Hempel equations. These equations are then expressed in the state space form [21,22] and will be referred to as Hill's equation and the Tschauner–Hempel equation, respectively. It is shown that they are null controllable with vanishing energy (NCVE) [23]. With this property, any state of the system can be steered to the origin with arbitrarily small amount of control energy in the L^2 (square integral) sense. The precise definition is given in the Appendix. This property guarantees that the L^2 norm of the feedback control obtained by the linear quadratic regulator theory can be made

arbitrarily small by choosing the penalty matrix on the state small. This property is exploited in the control design.

The relative orbit transfer problem is to find feedback controls, which steer the chaser in a given initial orbit to a given final orbit. Thus our problem is an infinite horizon problem with free end conditions. To find feedback controls, a "virtual spacecraft" is introduced in the final orbit and the error system is derived. To exploit the NCVE property, the relative orbit transfer problem is formulated as a linear quadratic regulator problem and an optimal feedback control based on the Riccati equation is obtained. The feedback control steers the chaser to the final orbit asymptotically. The optimal quadratic cost for Hill's equation is parametrized by the difference of initial conditions of the chaser and the virtual spacecraft. Thus it is further minimized with respect to the initial conditions, which yields the best position (initial condition) of the chaser and the best initial position of the virtual spacecraft. They are found analytically when the initial and final orbits are concentric ellipses or when they intersect. For the Tschauner–Hempel equation the feedback controller is constructed from the Riccati differential equation with periodic coefficients. The optimal quadratic cost in this case is parametrized by the initial condition of the true anomaly and is again minimized with respect to it.

Because both Hill's equation and the Tschauner–Hempel equation are NCVE, the control energy for the transfer evaluated in the L^2 sense can be made arbitrarily small. This is realized by choosing the weight parameters in the quadratic cost small. For rendezvous and formation flying, impulsive maneuvers are usually employed and their performance is evaluated by the total change of velocity denoted by ΔV_T [3]. For our feedback controls the control energy in the L^1 (absolute integral) sense corresponds to the total velocity change of impulsive maneuvers. Hence the L^1 norm of the feedback control is compared with ΔV_T.

For numerical simulations a circular orbit and an eccentric orbit of geostationary transfer orbit (GTO) type are considered. Linear feedback controls are designed in each case and applied to the original nonlinear equations of the chaser. Several performance indices are calculated. Simulation results indicate that feedback controllers with good performance can be designed. By employing multistage transfer, maximum values of feedback controls are significantly reduced.

The paper is organized as follows. Section II reviews Hill's equations and Tschauner–Hempel equations and shows their NCVE property. Section III formulates the relative orbit transfer problems along circular and eccentric orbits. The first half of the section is concerned with Hill's equation, and the transfer problem between two elliptic relative orbits, which are concentric or which intersect, is considered. As an example the circular orbit with height 500 km is considered. Feedback controllers with small L^1 norm are designed and simulation results are given. The second half of the section is concerned with an eccentric orbit of GTO type and the relative orbit transfer problem for the Tschauner–Hempel equation is considered. Feedback controllers with small L^1 norm are obtained and simulation results are presented. Section IV is the conclusion. In the Appendix the definitions of NCVE and CVE (controllability with vanishing energy) are given and their necessary and sufficient conditions are collected.

II. Equations of Relative Motion

Hill's equations describe the relative motion of the chaser with respect to the target. In this section the state space form of Hill's equations and its solution are briefly reviewed and the NCVE and CVE properties of the controlled Hill's equation are proved.

A. Hill's Equation

Consider the target spacecraft in a circular orbit of radius R_0 as shown in Fig. 1. The orbit rate in this case is given by $n = (\mu_e/R_0^3)^{1/2}$, where $\mu_e \equiv GM_e$ is the gravitational parameter of the Earth, G the universal gravitational constant, and M_e the mass of the Earth. To introduce Hill's equations, the right-handed coordinate system (x, y, z) fixed at the center of mass of the target is used, where x axis is along the radial direction, y axis along the flight direction of the target, and z axis is out of the orbit plane.

The Newton's equation of motion gives three equations

$$\ddot{x} = 2n\dot{y} + n^2(R_0 + x) - \frac{\mu_e(R_0 + x)}{[(R_0 + x)^2 + y^2 + z^2]^{\frac{3}{2}}} \tag{1}$$

$$\ddot{y} = -2n\dot{x} + n^2 y - \frac{\mu_e y}{[(R_0 + x)^2 + y^2 + z^2]^{\frac{3}{2}}} \tag{2}$$

$$\ddot{z} = -\frac{\mu_e z}{[(R_0 + x)^2 + y^2 + z^2]^{\frac{3}{2}}} \tag{3}$$

The linearized equations around the origin are given by

$$\ddot{x} = 2n\dot{y} + 3n^2 x \tag{4}$$

$$\ddot{y} = -2n\dot{x} \tag{5}$$

$$\ddot{z} = -n^2 z \tag{6}$$

which are known as Hill's equations or Clohessy–Wiltshire equations [1–4]. Note that Eq. (6) is independent of (4) and (5). Now introduce control accelerations u_x, u_y, and u_z to Eqs. (4–6), respectively. Then the state space equation for the resulting equations is

$$\dot{\boldsymbol{x}} = \begin{bmatrix} 0 & 0 & 1 & 0 & 0 & 0 \\ 0 & 0 & 0 & 1 & 0 & 0 \\ 3n^2 & 0 & 0 & 2n & 0 & 0 \\ 0 & 0 & -2n & 0 & 0 & 0 \\ 0 & 0 & 0 & 0 & 0 & 1 \\ 0 & 0 & 0 & 0 & -n^2 & 0 \end{bmatrix} \boldsymbol{x} + \begin{bmatrix} 0 & 0 & 0 \\ 0 & 0 & 0 \\ 1 & 0 & 0 \\ 0 & 1 & 0 \\ 0 & 0 & 0 \\ 0 & 0 & 1 \end{bmatrix} \boldsymbol{u}$$
$$\equiv A\boldsymbol{x} + B\boldsymbol{x} \tag{7}$$

where

$$\boldsymbol{x} = \begin{bmatrix} x & y & \dot{x} & \dot{y} & z & \dot{z} \end{bmatrix}', \qquad \boldsymbol{u} = \begin{bmatrix} u_x & u_y & u_z \end{bmatrix}'$$

and $(\cdot)'$ denotes the transpose. The system (7) will be referred to as the (controlled) Hill's equation. The transition matrix e^{At} is given by

$$e^{At} = \begin{bmatrix} 4 - 3\cos nt & 0 & (1/n)\sin nt & (2/n)(1 - \cos nt) & 0 & 0 \\ 6(\sin nt - nt) & 1 & (2/n)(\cos nt - 1) & (4/n)\sin nt - 3t & 0 & 0 \\ 3n\sin nt & 0 & \cos nt & 2\sin nt & 0 & 0 \\ 6n(\cos nt - 1) & 0 & -2\sin nt & 4\cos nt - 3 & 0 & 0 \\ 0 & 0 & 0 & 0 & \cos nt & \sin nt \\ 0 & 0 & 0 & 0 & -\sin nt & \cos nt \end{bmatrix} \tag{8}$$

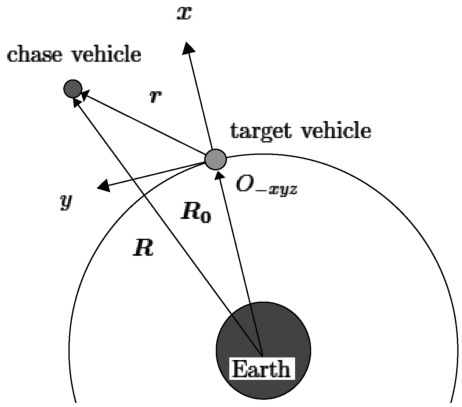

Fig. 1 Target in circular orbit.

This yields the solutions of the free motion

$$\begin{aligned} x(t) &= 4x_0 + (2/n)\dot{y}_0 - [3x_0 + (2/n)\dot{y}_0]\cos nt + (1/n)\dot{x}_0 \sin nt \\ y(t) &= y_0 - (2/n)\dot{x}_0 + (2/n)\dot{x}_0 \cos nt + [6x_0 + (4/n)\dot{y}_0]\sin nt \\ &\quad - (6nx_0 + 3\dot{y}_0)t \\ z(t) &= z_0 \cos nt + (1/n)\dot{z}_0 \sin nt \end{aligned} \tag{9}$$

It is easily seen from (9) that the solutions are periodic if and only if

$$\dot{y}_0 = -2nx_0 \tag{10}$$

In this case the same relation $\dot{y}(t) = -2nx(t)$ holds for all t. This follows from

$$\begin{cases} x(t) = x_0 \cos nt + (1/n)\dot{x}_0 \sin nt \\ y(t) = y_0 - (2/n)\dot{x}_0 + (2/n)\dot{x}_0 \cos nt - 2x_0 \sin nt \end{cases} \tag{11}$$

These equations are equivalently written in the form

$$\begin{cases} x(t) = a\sin(nt + \alpha) \\ y(t) = \bar{d} + 2a\cos(nt + \alpha) \end{cases}$$

where

$$\bar{d} \equiv y_0 - (2/n)\dot{x}_0, \qquad a \equiv \sqrt{x_0^2 + (\dot{x}_0/n)^2} \tag{12}$$

$$\cos\alpha = (\dot{x}_0/na), \qquad \sin\alpha = (x_0/a)$$

Hence, the trajectory of the periodic solutions (11) is an ellipse with center $(0, \bar{d})$ and eccentricity $e = (\sqrt{3}/2)$

$$\frac{x^2}{a^2} + \frac{(y-\bar{d})^2}{(2a)^2} = 1 \tag{13}$$

Hill's equation (7) is controllable and the eigenvalues of A are $\{0, 0, \pm ni, \pm ni\}$ and lie on the imaginary axis. Therefore the following result is a direct consequence of Theorems A1 and A2.

Theorem 2.1. Hill's equation (7) is CVE and hence NCVE.

The CVE property guarantees the state transfer of the system with arbitrarily small amount of energy. The subsystem describing the in-plane motion is

$$\dot{\boldsymbol{x}} = \begin{bmatrix} 0 & 0 & 1 & 0 \\ 0 & 0 & 0 & 1 \\ 3n^2 & 0 & 0 & 2n \\ 0 & 0 & -2n & 0 \end{bmatrix}\boldsymbol{x} + \begin{bmatrix} 0 & 0 \\ 0 & 0 \\ 1 & 0 \\ 0 & 1 \end{bmatrix}\boldsymbol{u}, \equiv A_1\boldsymbol{x} + B_1\boldsymbol{u} \tag{14}$$

which is also referred to as Hill's equation. Note that this is CVE (NCVE). Based on this property, a control strategy for the relative orbit transfer will be proposed in Sec. III.

B. Tschauner–Hempel Equation

Consider the target spacecraft in an eccentric orbit shown in Fig. 2. Here θ denotes the true anomaly and R_0 is the distance from the center of the Earth to the target. The equations of motion of the target are written as

$$\ddot{R}_0 - R_0\dot{\theta}^2 = -(\mu_e/R_0^2) \tag{15}$$

$$2\dot{R}_0\dot{\theta} + R_0\ddot{\theta} = 0 \tag{16}$$

Let T be the period of the eccentric orbit. Then the solutions of (15) and (16) are T periodic. The relative motion of the chaser with respect to the target is described by

$$\ddot{x} = \frac{\mu_e}{R_0^2} + \dot{\theta}^2 x - \frac{2\dot{R}_0\dot{\theta}}{R_0}y + 2\dot{\theta}\dot{y} - \frac{\mu_e(R_0+x)}{[(R_0+x)^2 + y^2 + z^2]^{\frac{3}{2}}} \tag{17}$$

$$\ddot{y} = \frac{2\dot{R}_0\dot{\theta}}{R_0}x - 2\dot{\theta}\dot{x} + \ddot{\theta}^2 y - \frac{\mu_e y}{[(R_0+x)^2 + y^2 + z^2]^{\frac{3}{2}}} \tag{18}$$

$$\ddot{z} = -\frac{\mu_e z}{[(R_0+x)^2 + y^2 + z^2]^{\frac{3}{2}}} \tag{19}$$

The linearization around the origin yields

$$\ddot{x} = \left(\dot{\theta}^2 + 2\frac{\mu_e}{R_0^3}\right)x - \frac{2\dot{R}_0\dot{\theta}}{R_0}y + 2\dot{\theta}\dot{y} \tag{20}$$

$$\ddot{y} = \frac{2\dot{R}_0\dot{\theta}}{R_0}x + \left(\dot{\theta}^2 - \frac{\mu_e}{R_0^3}\right)y - 2\dot{\theta}\dot{x} \tag{21}$$

$$\ddot{z} = -\frac{\mu_e}{R_0^3}z \tag{22}$$

which are known as Tschauner–Hempel equations. If $\dot{\theta} = n$, these equations are reduced to (4–6). The state space form of the controlled equations is

$$\begin{aligned} \dot{\boldsymbol{x}} &= \begin{bmatrix} 0 & 0 & 1 & 0 & 0 & 0 \\ 0 & 0 & 0 & 1 & 0 & 0 \\ \dot{\theta}^2 + 2\frac{\mu_e}{R_0^3} & -\frac{2\dot{R}_0\dot{\theta}}{R_0} & 0 & 2\dot{\theta} & 0 & 0 \\ \frac{2\dot{R}_0\dot{\theta}}{R_0} & \dot{\theta}^2 - \frac{\mu_e}{R_0^3} & -2\dot{\theta} & 0 & 0 & 0 \\ 0 & 0 & 0 & 0 & 0 & 1 \\ 0 & 0 & 0 & 0 & -\frac{\mu_e}{R_0^3} & 0 \end{bmatrix}\boldsymbol{x} + \begin{bmatrix} 0 & 0 & 0 \\ 0 & 0 & 0 \\ 1 & 0 & 0 \\ 0 & 1 & 0 \\ 0 & 0 & 0 \\ 0 & 0 & 1 \end{bmatrix}\boldsymbol{u} \\ &\equiv A(t)\boldsymbol{x} + B\boldsymbol{u} \end{aligned} \tag{23}$$

where $A(t)$ is T periodic. This system is referred to as the (controlled) Tschauner–Hempel equation. It is an easy exercise to show that $[A(t), B]$ is controllable. Below the CVE property of $[A(t), B]$ will be shown. Because the system (20) and (21) and the system (22) are independent, it is enough to show that these two subsystems are CVE. First consider the system describing the in-plane motion

$$\begin{aligned} \dot{\boldsymbol{x}} &= \begin{bmatrix} 0 & 0 & 1 & 0 \\ 0 & 0 & 0 & 1 \\ \dot{\theta}^2 + 2\frac{\mu_e}{R_0^3} & -\frac{2\dot{R}_0\dot{\theta}}{R_0} & 0 & 2\dot{\theta} \\ \frac{2\dot{R}_0\dot{\theta}}{R_0} & \dot{\theta}^2 - \frac{\mu_e}{R_0^3} & -2\dot{\theta} & 0 \end{bmatrix}\boldsymbol{x} + \begin{bmatrix} 0 & 0 \\ 0 & 0 \\ 1 & 0 \\ 0 & 1 \end{bmatrix}\boldsymbol{u} \\ &\equiv A_1(t)\boldsymbol{x} + B_1\boldsymbol{u} \end{aligned} \tag{24}$$

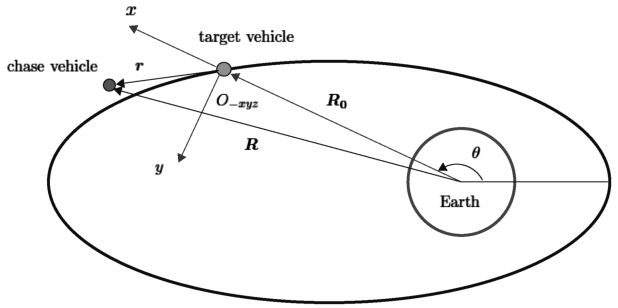

Fig. 2 Target in eccentric orbit.

Let $0 \le t_0 < T$. The solution of (24) with $\boldsymbol{u} = 0$ and $\boldsymbol{x}(\boldsymbol{t_0}) = \boldsymbol{x_0}$ is obtained from Yamanaka and Ankerson [19] as follows:

$$\boldsymbol{x} = \Phi_\theta K \tag{25}$$

where

$$\boldsymbol{x} = \begin{bmatrix} x & y & \dot{x} & \dot{y} \end{bmatrix}', \qquad K = \begin{bmatrix} k_1 & k_2 & k_3 & k_4 \end{bmatrix}'$$

$$\Phi_\theta = \begin{bmatrix} 0 & -\frac{s}{\rho} & -\frac{c}{\rho} & -\frac{1}{\rho}(2-3esG) \\ \frac{1}{\rho} & -\frac{c}{\rho}\left(1+\frac{1}{\rho}\right) & \frac{s}{\rho}\left(1+\frac{1}{\rho}\right) & 3\rho G \\ 0 & -\frac{\dot\theta}{\rho}c & \frac{\dot\theta}{\rho}s & \frac{\dot\theta}{\rho}e\left(3cG+\frac{s}{\rho^2}\right) \\ \frac{es\dot\theta}{\rho^3} & \frac{s\dot\theta}{\rho^2}\left[2+e\frac{c}{\rho}\left(1-\frac{1}{\rho}\right)\right] & \frac{\dot\theta}{\rho}\left[c\left(1+\frac{1}{\rho}\right)+e\frac{s^2}{\rho^3}\right] & 3\frac{\dot\theta}{\rho}(1-esG) \end{bmatrix}$$

$$\rho = 1 + e\cos\theta, \quad c = \rho\cos\theta, \quad s = \rho\sin\theta$$

$$k^2(t-t_0) = \int_{\theta_0}^{\theta} \frac{1}{\rho(\tau)^2} d\tau = G(\theta), \quad k = \frac{\mu_e}{h^3} \tag{26}$$

$\theta_0 = \theta(t_0)$ and h is the orbital angular momentum of the target spacecraft. Because $G(\theta_0) = 0$ by (26), it leads to

$$\Phi_{\theta_0} = \begin{bmatrix} 0 & -\frac{s}{\rho} & -\frac{c}{\rho} & -\frac{2}{\rho} \\ \frac{1}{\rho} & -\frac{c}{\rho}\left(1+\frac{1}{\rho}\right) & \frac{s}{\rho}\left(1+\frac{1}{\rho}\right) & 0 \\ 0 & -\frac{\dot\theta}{\rho}c & \frac{\dot\theta}{\rho}s & \frac{s\dot\theta e}{\rho^3} \\ \frac{es\dot\theta}{\rho^3} & \frac{s\dot\theta}{\rho^2}\left[2+e\frac{c}{\rho}\left(1-\frac{1}{\rho}\right)\right] & \frac{\dot\theta}{\rho}\left[c\left(1+\frac{1}{\rho}\right)+e\frac{s^2}{\rho^3}\right] & 3\frac{\dot\theta}{\rho} \end{bmatrix}_{\theta_0}$$

From $0 \le e < 1$, it follows that $\det \Phi_{\theta_0} \neq 0$. Now K is determined by

$$K = \Phi_{\theta_0}^{-1} \boldsymbol{x}(t_0) \tag{27}$$

and (25) is rewritten as

$$\boldsymbol{x}(t) = \Phi_\theta \Phi_{\theta_0}^{-1} \boldsymbol{x}_0$$

Therefore

$$S_1(t, t_0) = \Phi_{\theta(t)} \Phi_{\theta_0(t_0)}^{-1}$$

where $S_1(t, t_0)$ is the transition matrix corresponding to $A_1(t)$. Because $G(\theta)$ is the only aperiodic component in Φ_θ, $x(t)$ and $y(t)$ become periodic if $k_4 = 0$. In this case

$$\begin{cases} x(t) = -k_2\sin\theta - k_3\cos\theta \\ y(t) = (1/\rho)k_1 - (c/\rho)[1+(1/\rho)]k_2 + (s/\rho)[1+(1/\rho)]k_3 \end{cases} \tag{28}$$

and its trajectory is written as

$$\frac{x^2}{k_2^2 + k_3^2} + \frac{[y - (k_1/\rho)]^2}{[1+(1/\rho)]^2(k_2^2+k_3^2)} = 1$$

Hence, the parameter K determines the shape of the periodic solution. If K and θ_0 are given, then $\boldsymbol{x}(t_0)$ is determined uniquely by (27). Now the CVE (NCVE) property of (23) is examined. Note that $S_1(T+t_0, t_0) = S_1(t_0, 0)S_1(T, 0)S_1(t_0, 0)^{-1}$. Therefore $S_1(T+t_0, t_0)$ and $S_1(T, 0)$ are similar and have the same eigenvalues. Below the set of eigenvalues of $S_1(T, 0)$ are identified with $\{1, 1, 1, 1\}$. Now

$$S_1(T,0) = \Phi_{\theta(T)}\Phi_{\theta(0)}^{-1} = (\Phi_{\theta(0)} + \Delta\Phi)\Phi_{\theta(0)}^{-1} = \begin{bmatrix} 1 & 0 & 0 & 0 \\ * & 1 & 0 & * \\ * & 0 & 1 & * \\ 0 & 0 & 0 & 1 \end{bmatrix}$$

where

$$\Delta\Phi = \begin{bmatrix} 0 & 0 & 0 & 0 \\ 0 & 0 & 0 & 3(1+e)k^2T \\ 0 & 0 & 0 & \dot\theta(T)\frac{3e}{1+e}k^2T \\ 0 & 0 & 0 & 0 \end{bmatrix}$$

$$\Phi_{\theta(0)} = \begin{bmatrix} 0 & 0 & -1 & -\frac{2}{1+e} \\ \frac{1}{1+e} & -\frac{2+e}{1+e} & 0 & 0 \\ 0 & -\frac{\dot\theta(T)}{1+e} & 0 & 0 \\ 0 & \frac{e^2}{(1+e)^2} & \frac{\dot\theta(T)(2+e)}{(1+e)^2} & \frac{3\dot\theta(T)}{1+e} \end{bmatrix}$$

A direct computation shows that the last row of $\Phi_{\theta(0)}^{-1}$ is of the form $[\,*\ \ 0\ \ 0\ \ *\,]$ where $*$ denotes some nonzero numbers. Thus $\sigma[S_1(T,0)] = \{1,1,1,1\}$. This property is also discussed in [20]. It follows from Theorem A4 that the system (23) is CVE.

The subsystem for the out-of-plane motion is given by

$$\dot{\boldsymbol{x}} = \begin{bmatrix} 0 & 1 \\ -\frac{\mu_e}{R_0^3} & 0 \end{bmatrix}\boldsymbol{x} + \begin{bmatrix} 0 \\ 1 \end{bmatrix}\boldsymbol{u}, \equiv A_2(t)\boldsymbol{x} + B_2\boldsymbol{u}$$

Using the solution

$$z(t) = (1/\rho)(k_1\cos\theta + k_2\sin\theta)$$

the identity $\sigma[S_2(T,0)] = \{1,1\}$ can be shown in a similar manner, where $S_2(t,s)$ is the transition matrix associated with $A_2(t)$. Hence the following result is proved.

Theorem 2.2. The Tschauner–Hempel equation (23) is CVE and hence NCVE on any interval $[t_0, \infty)$, $0 \le t_0 < T$.

III. Relative Orbit Transfer

As discussed in Sec. II, Hill's equation (7) and the Tschauner–Hempel equation (23) have periodic solutions (11) and (28), respectively. They are relative orbits of the chaser. If the periodic solutions encircle the target spacecraft in the orbit plane, then passive flyaround could be fulfilled by putting the chaser into these orbits.

In this section the relative orbit transfer problem from a given orbit to another is considered. Because the in-plane motion and the out-of-plane motion are independent, only the in-plane motion, which is more involved, will be discussed. Feedback controllers based on the linear quadratic regulator theory and the NCVE property are proposed.

A. Relative Orbit Transfer Along a Circular Orbit

Recall that Hill's equations (4) and (5) give elliptic relative orbits (11) and (13) of the chaser. Let

$$\begin{cases} \frac{x^2}{a_1^2} + \frac{(y-\bar d_1)^2}{(2a_1)^2} = 1 & \text{(initial orbit)} \\ \frac{x^2}{a_2^2} + \frac{(y-\bar d_2)^2}{(2a_2)^2} = 1 & \text{(final orbit)} \end{cases}$$

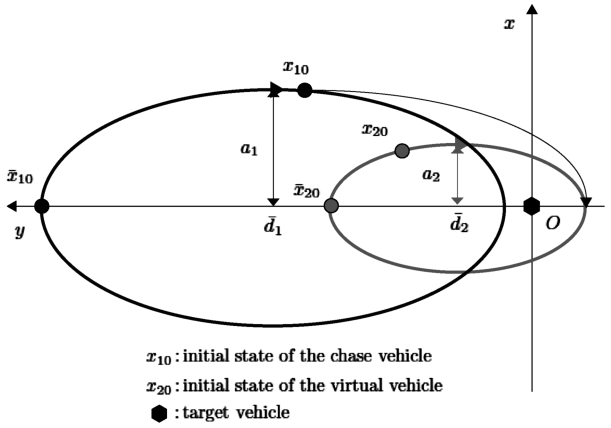

Fig. 3 Relative orbit transfer.

be the initial and final relative orbits of the chaser, respectively, given in Fig. 3, where O is the origin which indicates the position of the target in the (x, y) frame, the parameter a denotes the semiminor axis of the relative orbit and the parameter $\bar{d}$ denotes the distance from the target spacecraft to the center of the relative orbit. Note that the orbits in Fig. 3 are not orbits in the inertial frame. Assume that the chaser in the beginning is in free motion and in the initial orbit, which is the larger elliptic orbit. Consider the problem of finding a feedback control, which steers the chaser asymptotically to the final orbit, which is the smaller elliptic orbit in Fig. 3. This problem could be interpreted as the transfer from a temporary relative orbit to a relative orbit for inspection. Let $\boldsymbol{x}_{10} = \begin{bmatrix} x_0 & y_0 & \dot{x}_0 & \dot{y}_0 \end{bmatrix}'$ be the initial condition of the chaser so that (x_0, y_0) satisfies (13) and the conditions (10) and (12) hold for $a = a_1$ and $\bar{d} = \bar{d}_1$. Recall Hill's equation (1)

$$\dot{\boldsymbol{x}}_1 = A_1 \boldsymbol{x}_1 + B\boldsymbol{u}, \qquad \boldsymbol{x}_1(0) = \boldsymbol{x}_{10}$$

If $\boldsymbol{u} = 0$, then the chaser stays in the initial relative orbit for all time. It is convenient to introduce a virtual spacecraft in the final orbit given by

$$\dot{\boldsymbol{x}}_2 = A_1 \boldsymbol{x}_2, \qquad \boldsymbol{x}_2(0) = \boldsymbol{x}_{20}$$

where $\boldsymbol{x}_{20}$ is the initial condition of the virtual spacecraft that satisfies (10), (12), and (13) with $a = a_2$ and $\bar{d} = \bar{d}_2$. Thus the virtual spacecraft stays in the final orbit for all time. To find a desired feedback control, introduce the system for the error $\boldsymbol{x} \equiv \boldsymbol{x}_1 - \boldsymbol{x}_2$

$$\dot{\boldsymbol{x}} = A_1 \boldsymbol{x} + B\boldsymbol{u}, \qquad \boldsymbol{x}(0) = \boldsymbol{x}_0$$

where $\boldsymbol{x}_0 \equiv \boldsymbol{x}_{10} - \boldsymbol{x}_{20}$. Now a feedback control is designed via the linear quadratic regulator problem [21,22] that minimizes the cost function

$$J(\boldsymbol{u}; \boldsymbol{x}_0) = \int_0^\infty [\boldsymbol{x}(t)' Q \boldsymbol{x}(t) + \boldsymbol{u}(t)' R \boldsymbol{u}(t)]\, \mathrm{d}t$$

where $Q \geq 0$, $R > 0$ and (C, A) with $C = \sqrt{Q}$ is assumed to be observable. Because (A, B) is controllable, there exists a unique positive definite stabilizing solution of the algebraic Riccati equation (ARE)

$$A'X + XA - XBR^{-1}B'X + Q = 0 \tag{29}$$

The optimal control is given by the stabilizing feedback control

$$\boldsymbol{u}^*(t) = -R^{-1}B'X\boldsymbol{x}(t) \tag{30}$$

and the minimum cost by

$$\hat{J}(\boldsymbol{x}_0) \equiv J(\boldsymbol{u}^*, \boldsymbol{x}_0) = \boldsymbol{x}_0' X \boldsymbol{x}_0 \tag{31}$$

Because the feedback controller (30) is stabilizing, $\boldsymbol{x}(t) \to 0$ as $t \to \infty$. Hence, the chaser approaches the final orbit asymptotically. If $a_2 = \bar{d}_2 = 0$, then the final orbit collapses to the origin and it corresponds to the rendezvous and docking (of the point mass systems). Because the relative orbit transfer problem is at stake, the time to introduce control inputs to the equation of motion of the chaser is assumed free. This implies that the initial condition $\boldsymbol{x}_{10}$ could be any point satisfying (10), (12), and (13) with $a = a_1$ and $\bar{d} = \bar{d}_1$. The initial condition $\boldsymbol{x}_{20}$ is also an arbitrary point satisfying (10), (12), and (13) with $a = a_2$ and $\bar{d} = \bar{d}_2$. Therefore it is useful to minimize $\hat{J}(\boldsymbol{x}_0)$ with respect to $\boldsymbol{x}_{10}$ and $\boldsymbol{x}_{20}$ and to find the best initial positions of the chaser and the virtual spacecraft. For this purpose consider the special points

$$\begin{aligned} \bar{\boldsymbol{x}}_{10} &= \begin{bmatrix} 0 & \bar{d}_1 + 2a_1 & na_1 & 0 \end{bmatrix}' \\ \bar{\boldsymbol{x}}_{20} &= \begin{bmatrix} 0 & \bar{d}_2 + 2a_2 & na_2 & 0 \end{bmatrix}' \end{aligned} \tag{32}$$

Note that these points correspond to those on the major axes of initial and final orbits, respectively, see Fig. 3. It is easy to parametrize the initial conditions $\boldsymbol{x}_{10}$ and $\boldsymbol{x}_{20}$ as follows:

$$\boldsymbol{x}_{10} = e^{A\tau_1}\bar{\boldsymbol{x}}_{10} \qquad [0 \leq \tau_1 < (2\pi/n)] \qquad \boldsymbol{x}_{20} = e^{A\tau_2}\bar{\boldsymbol{x}}_{20} \qquad [0 \leq \tau_2 < (2\pi/n)] \tag{33}$$

Now $\hat{J}(\boldsymbol{x}_0)$ is given by

$$\hat{J} = (e^{A\tau_1}\bar{\boldsymbol{x}}_{10} - e^{A\tau_2}\bar{\boldsymbol{x}}_{20})' X (e^{A\tau_1}\bar{\boldsymbol{x}}_{10} - e^{A\tau_2}\bar{\boldsymbol{x}}_{20}) \tag{34}$$

Thus the minimization of $\hat{J}$ with respect to $\boldsymbol{x}_0$ is reduced to the minimization with respect to τ_1 and τ_2, which will be discussed below.

1. Transfer Between Concentric Elliptic Orbits

Here the special case $d \equiv \bar{d}_1 - \bar{d}_2 = 0$ is considered, where the initial and final orbits are concentric ellipses. Substituting (8) and (33) into (34), $\boldsymbol{x}_{10}$ and $\boldsymbol{x}_{20}$ are written as

$$\boldsymbol{x}_{10} = \begin{bmatrix} a_1 \sin n\tau_1 \\ \bar{d}_1 + 2a_1 \cos n\tau_1 \\ na_1 \cos n\tau_1 \\ -2na_1 \sin n\tau_1 \end{bmatrix}, \qquad \boldsymbol{x}_{20} = \begin{bmatrix} a_2 \sin n\tau_2 \\ \bar{d}_2 + 2a_2 \cos n\tau_2 \\ na_2 \cos n\tau_2 \\ -2na_2 \sin n\tau_2 \end{bmatrix}$$

so that

$$\boldsymbol{x}_0 = \begin{bmatrix} a_1 \sin n\tau_1 - a_2 \sin n\tau_2 \\ 2(a_1 \cos n\tau_1 - a_2 \cos n\tau_2) \\ n(a_1 \cos n\tau_1 - a_2 \cos n\tau_2) \\ -2n(a_1 \sin n\tau_1 - a_2 \sin n\tau_2) \end{bmatrix}$$

To minimize (34) it is convenient to introduce

$$\begin{bmatrix} \xi \\ \eta \end{bmatrix} = \begin{bmatrix} \cos n\tau_1 & -\cos n\tau_2 \\ \sin n\tau_1 & -\sin n\tau_2 \end{bmatrix} \begin{bmatrix} a_1 \\ a_2 \end{bmatrix} \tag{35}$$

Then $\boldsymbol{x}_0$ is expressed as

$$\boldsymbol{x}_0' = \begin{bmatrix} \eta & 2\xi & n\xi & -2n\eta \end{bmatrix} \tag{36}$$

Because X is positive definite, we write

$$X = \begin{bmatrix} X_{11} & X_{12} & X_{13} & X_{14} \\ X_{12} & X_{22} & X_{23} & X_{24} \\ X_{13} & X_{23} & X_{33} & X_{34} \\ X_{14} & X_{24} & X_{34} & X_{44} \end{bmatrix}$$

Then $\hat{J}$ is given by

$$\hat{J} = \boldsymbol{x}_0' X \boldsymbol{x}_0 = (4X_{22} + 4nX_{23} + n^2X_{33})\xi^2 + 2(2X_{12} + nX_{13} - 4nX_{24} - 2n^2X_{34})\xi\eta + (X_{11} - 4nX_{14} + 4n^2X_{44})\eta^2 = \begin{bmatrix} \xi & \eta \end{bmatrix} P \begin{bmatrix} \xi \\ \eta \end{bmatrix} > 0 \tag{37}$$

for any $\boldsymbol{x}_0 \neq 0$, where $P = (P_{ij})$ is a symmetric matrix with

$$P_{11} = 4X_{22} + 4nX_{23} + n^2X_{33}$$
$$P_{12} = 2X_{12} + nX_{13} - 4nX_{24} - 2n^2X_{34}$$
$$P_{22} = X_{11} - 4nX_{14} + 4n^2X_{44}$$

In view of (36) and (37) P is positive definite. Thus in the (ξ, η) plane, $\hat{J} = \text{const}$ describes an ellipse with center at the origin. The region where (ξ, η) traverses can be found as follows. The definition (35) gives

$$\xi^2 + \eta^2 = a_1^2 + a_2^2 - 2a_1a_2 \cos n(\tau_1 - \tau_2) \equiv r^2(\tau_1, \tau_2) \tag{38}$$

and the inequalities

$$(a_1 - a_2)^2 \leq r^2(\tau_1, \tau_2) \leq (a_1 + a_2)^2$$

Thus (38) describes a family of circles and (ξ, η) lies between two circles of radii $|a_1 - a_2|$ and $a_1 + a_2$; see Fig. 4. When $\tau_1 = \tau_2$, the radius takes the minimum value $|a_1 - a_2|$. In this case

$$\begin{cases} \xi = (a_1 - a_2)\cos n\tau_1 \\ \eta = (a_1 - a_2)\sin n\tau_1 \end{cases} \tag{39}$$

and (ξ, η) covers the whole circle. Therefore, as shown in Fig. 4, $\hat{J}$ takes the minimum value when the ellipse contacts the inner circle.

To find the minimizing τ_1 explicitly, let λ_1^2 and λ_2^2 be the eigenvalues of P, and $\boldsymbol{u_1}$ and $\boldsymbol{u_2}$ the corresponding normalized eigenvectors. Introduce the transformation

$$\begin{bmatrix} \xi \\ \eta \end{bmatrix} = \begin{bmatrix} \boldsymbol{u_1} & \boldsymbol{u_1} \end{bmatrix} \begin{bmatrix} \tilde{\xi} \\ \tilde{\eta} \end{bmatrix}$$

to obtain a simple expression

$$\hat{J} = \lambda_1^2\tilde{\xi}^2 + \lambda_2^2\tilde{\eta}^2$$

The ellipse $\hat{J} = k^2$ becomes

$$\frac{\tilde{\xi}^2}{(k/\lambda_1)^2} + \frac{\tilde{\eta}^2}{(k/\lambda_2)^2} = 1 \tag{40}$$

The minimum of $\hat{J}$ is attained at the points of contact of the ellipse (40) and the circle (39) shown in Fig. 4. Let $\lambda_1^2 < \lambda_2^2$ and set $\boldsymbol{u_1}' = [u_{11} \quad u_{21}]$. Then in view of (35) the minimizing τ_1 are given by

$$\tau_1^* = \begin{cases} \frac{1}{n}\tan^{-1}\left(\frac{u_{21}}{u_{11}}\right) & \in \left[0, \frac{\pi}{n}\right] \\ \frac{1}{n}\tan^{-1}\left(\frac{u_{21}}{u_{11}}\right) + \frac{\pi}{n} & \in \left[\frac{\pi}{n}, \frac{2\pi}{n}\right] \end{cases}$$

If $\lambda_1^2 = \lambda_2^2$, (40) describes a circle and any $\tau_1 (0 \leq \tau_1 < \frac{2\pi}{n})$ is a minimizing point.

2. *Transfer Between Arbitrary Elliptic Orbits*

Here the general case $d = \bar{d}_1 - \bar{d}_2 \neq 0$ is considered. Then $\boldsymbol{x}_0$ is written as

$$\boldsymbol{x}_0 = \begin{bmatrix} a_1 \sin n\tau_1 - a_2 \sin n\tau_2 \\ d + 2(a_1 \cos n\tau_1 - a_2 \cos n\tau_2) \\ n(a_1 \cos n\tau_1 - a_2 \cos n\tau_2) \\ -2n(a_1 \sin n\tau_1 - a_2 \sin n\tau_2) \end{bmatrix}$$

so that (37) becomes

$$\hat{J} = \begin{bmatrix} \xi - \bar{\xi} & \eta - \bar{\eta} \end{bmatrix} \begin{bmatrix} P_{11} & P_{12} \\ P_{12} & P_{22} \end{bmatrix} \begin{bmatrix} \xi - \bar{\xi} \\ \eta - \bar{\eta} \end{bmatrix} - \hat{k}_0$$

where

$$\bar{\xi} = \frac{-d[P_{22}(2X_{22} + nX_{23}) - P_{12}(X_{12} - 2nX_{24})]}{P_{11}P_{22} - P_{12}^2}$$
$$\bar{\eta} = \frac{-d[-P_{12}(2X_{22} + nX_{23}) + P_{22}(X_{12} - 2nX_{24})]}{P_{11}P_{22} - P_{12}^2}$$
$$\hat{k}_0 = -X_{22}d^2 + P_{11}\bar{\xi}^2 + 2P_{12}\bar{\xi}\,\bar{\eta} + P_{22}\bar{\eta}^2$$

$\hat{J} = \hat{k}^2 - \hat{k}_0$ describes an ellipse with center $(\bar{\xi}, \bar{\eta})$ (see Fig. 5). $\hat{J}$ takes the minimum value if and only if $\hat{k}^2$ is minimum. To find the minimum three cases below should be examined:

1) $\bar{\xi}^2 + \bar{\eta}^2 < (a_1 - a_2)^2$,
2) $(a_1 - a_2)^2 \leq \bar{\xi}^2 + \bar{\eta}^2 \leq (a_1 + a_2)^2$,
3) $(a_1 + a_2)^2 < \bar{\xi}^2 + \bar{\eta}^2$.

In cases 1 or 3, optimal pairs (τ_1^*, τ_2^*) exist but they are not analytically found. Therefore case 2 will be studied below. In this case $(\xi, \eta) = (\bar{\xi}, \bar{\eta})$ gives the minimum $\hat{J} = -\hat{k}_0 (\hat{k} = 0)$. The equality

$$\bar{\xi}^2 + \bar{\eta}^2 = a_1^2 + a_2^2 - 2a_1a_2 \cos[n(\tau_1^* - \tau_2^*)]$$

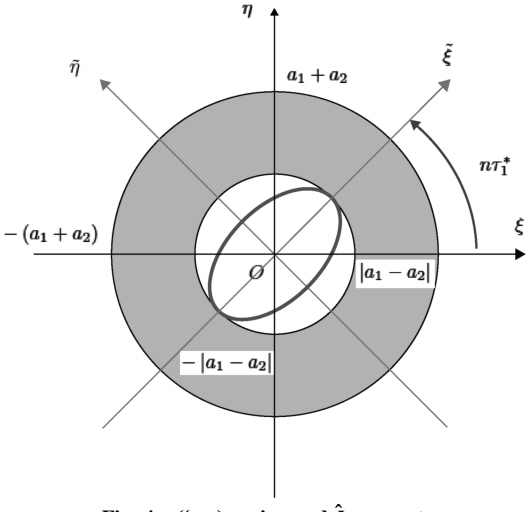

Fig. 4 (ξ, η) region and $\hat{J} = \text{const}$.

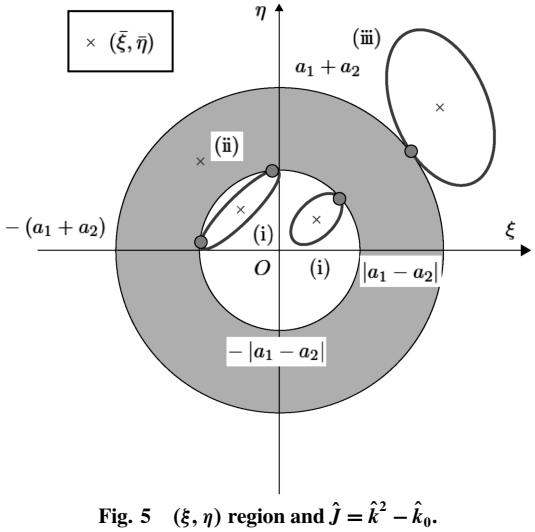

Fig. 5 (ξ, η) region and $\hat{J} = \hat{k}^2 - \hat{k}_0$.

implies

$$|\tau_1^* - \tau_2^*| = \frac{1}{n}\cos^{-1}\left[\frac{(a_1^2 + a_2^2) - (\bar{\xi}^2 + \bar{\eta}^2)}{2a_1 a_2}\right]$$

Define $\hat{\theta}$ as

$$\hat{\theta} = \cos^{-1}\left[\frac{(a_1^2 + a_2^2) - (\bar{\xi}^2 + \bar{\eta}^2)}{2a_1 a_2}\right] \qquad (0 \le \hat{\theta} < \pi) \qquad (41)$$

If $\tau_1^* \ge \tau_2^*$, then $\tau_1^* - \tau_2^* = (\hat{\theta}/n)$ and

$$\begin{aligned}\bar{\xi} &= a_1 \cos n\tau_1^* - a_2 \cos n\tau_2^* \quad = a_1 \cos(n\tau_2^* + \hat{\theta}) - a_2 \cos n\tau_2^* \\ &= (a_1 \cos\hat{\theta} - a_2)\cos n\tau_2^* - a_1 \sin\hat{\theta} \sin n\tau_2^* \\ &= (\bar{\xi}^2 + \bar{\eta}^2)^{\frac{1}{2}} \cos(n\tau_2^* + \theta_1) \end{aligned} \qquad (42)$$

where

$$\cos\theta_1 = \frac{a_1 \cos\hat{\theta} - a_2}{(\bar{\xi}^2 + \bar{\eta}^2)^{\frac{1}{2}}}, \qquad \sin\theta_1 = \frac{a_1 \sin\hat{\theta}}{(\bar{\xi}^2 + \bar{\eta}^2)^{\frac{1}{2}}}$$

and for the fourth equality, (41) is used. Similarly, $\bar{\eta}$ is written as

$$\bar{\eta} = (\bar{\xi}^2 + \bar{\eta}^2)^{\frac{1}{2}} \sin(n\tau_2^* + \theta_1) \qquad (43)$$

Hence in view of (42) and (43)

$$\begin{cases} \tau_1^* = \frac{1}{n}\left[\tan^{-1}\left(\frac{\bar{\eta}}{\bar{\xi}}\right) - \theta_1\right] + \frac{\hat{\theta}}{n} & \left(0 \le \tau_1^* < \frac{2\pi}{n}\right) \\ \tau_2^* = \frac{1}{n}\left[\tan^{-1}\left(\frac{\bar{\eta}}{\bar{\xi}}\right) - \theta_1\right] & \left(0 \le \tau_2^* < \frac{2\pi}{n}\right) \end{cases}$$

On the other hand, if $\tau_2^* \ge \tau_1^*$, then $\tau_2^* - \tau_1^* = (\hat{\theta}/n)$ and

$$\bar{\xi} = (\bar{\xi}^2 + \bar{\eta}^2)^{\frac{1}{2}} \cos(n\tau_1^* - \theta_2), \qquad \bar{\eta} = (\bar{\xi}^2 + \bar{\eta}^2)^{\frac{1}{2}} \sin(n\tau_1^* - \theta_2)$$

where

$$\cos\theta_2 = \frac{a_1 - a_2 \cos\hat{\theta}}{(\bar{\xi}^2 + \bar{\eta}^2)^{\frac{1}{2}}}, \qquad \sin\theta_2 = \frac{a_2 \sin\hat{\theta}}{(\bar{\xi}^2 + \bar{\eta}^2)^{\frac{1}{2}}}$$

Hence in this case

$$\begin{cases} \tau_1^* = \frac{1}{n}\left[\tan^{-1}\left(\frac{\bar{\eta}}{\bar{\xi}}\right) + \theta_2\right] & \left(0 \le \tau_1^* < \frac{2\pi}{n}\right) \\ \tau_2^* = \frac{1}{n}\left[\tan^{-1}\left(\frac{\bar{\eta}}{\bar{\xi}}\right) + \theta_2\right] + \frac{\hat{\theta}}{n} & \left(0 \le \tau_2^* < \frac{2\pi}{n}\right) \end{cases}$$

In the developments above, the weight matrices Q and R are fixed and the following problem is considered: $\min_{x_0} \min_u J(u; \boldsymbol{x}_0)$. But in applications it is desirable to keep the L^2 norm of the feedback control (30) small. For this purpose one could take $Q = qI$ for example and let $q \to 0$. Then the solution X_q of (29) approaches the solution of (A2), which is zero. Hence the orbit transfer can be realized by the feedback with arbitrarily small L^2 norm. However, the settling time becomes larger. For rendezvous and formation flying, impulse maneuvers are often employed and their performance is evaluated by the total velocity change required for the maneuver. For continuous controls the L^1 norm corresponds to this. As the L^2 norm of the feedback decreases to zero, the L^1 norm in general decreases and approaches to a positive constant. This will be confirmed by the simulation results below. This phenomenon concerning open loop controls is observed and analyzed for infinite dimensional systems [24].

Table 1 Constants and parameters of circular orbit

Constants	Values
R_e	6378.136 km
μ_e	398, 601 km^3/s^2
Common parameters	Values
h	500 km
n	1.1068×10^{-3} rad/s
T	5677 s

3. Simulation Results

For numerical simulations the circular orbit of the target spacecraft of height $h = 500$ km is considered. The period of this orbit is $T = 5677$ s and the orbit rate $n = 1.1068 \times 10^{-3}$ rad/s; see Table 1, where the radius of the Earth R_e and the gravitational constant of the Earth μ_e are also given.

To see that (7) is NCVE, the initial condition $\boldsymbol{x}_0 = [0 \quad \bar{d} + 2a \quad na \quad 0]$, with $\bar{d} = 0$, $a = 50$ is taken. This corresponds to the one of the points on the major axis of the relative orbit with center at the origin and semiminor axis $a = 50$. The norm $\|\hat{\boldsymbol{u}}\|_{L^2(0,T_f;\boldsymbol{R}^m)}$ of the control

$$\hat{\boldsymbol{u}} = -B' e^{A'(T_f - t)} Q_{T_f}^{-1} e^{AT_f} \boldsymbol{x}_0 \qquad Q_{T_f} = \int_0^{T_f} e^{A(T_f - t)} BB' e^{A'(T_f - t)}\, \mathrm{d}t$$

which steers $\boldsymbol{x}_0$ to the origin at time T_f with minimum L^2 norm, is plotted in Fig. 6. The norm decreases toward zero as time T_f tends to infinity.

To consider the orbit transfer problem, two concentric elliptic relative orbits of Hill's equation are chosen. The center of the two ellipses is at the origin (at the target vehicle) and the semiminor axes of the initial and final orbits are 50 km and 5 km, respectively, see Table 2, where CSS stands for "concentric" and "single stage."

To design a feedback controller, Q in the ARE (29) is chosen small relative to R so that the L^2 norm of the feedback controller becomes sufficiently small. For simplicity the matrices Q and R in (29) are assumed diagonal, that is, $Q = \mathrm{diag}(q_i)$ and $R = \mathrm{diag}(r_i)$. From the computational point of view, it is assumed that $q_i \ll 1$ and $r_i \gg 1$. Then the L^2 norm of the feedback controller can be made arbitrarily small. For the simulation these parameters are set $q_i = 1.0 \times 10^{-9}$, $i = 1, 2$, $q_i = 0$, $i = 3, 4$, and $r_i = 1.0 \times 10^5$. The feedback controller (30) has been applied to the nonlinear Hill's equations (1) and (2) with control u_x and u_y. To introduce a stopping rule, let $r_{\min}$ denote the minimum distance of a point in the final orbit from its center, and $v_{\min}$ the minimum velocity of the chaser in the final orbit. The chaser is regarded in the final orbit if $|x|, |y| < 0.01 r_{\min}$ and $|\dot{x}|, |\dot{y}| < 0.01 v_{\min}$. The controlled trajectory of the chaser is depicted in Fig. 7 and the control inputs in Fig. 8. The settling time $T_s = 37546$ s and the L^2 norm of the control is 3.1446×10^{-1} m/s$^{\frac{3}{2}}$.

The relative orbit transfer could be done by the two-impulse maneuver shown in Fig. 9 and the total velocity change $\Delta V_T = 49.805$ m/s. The L^1 norm for continuous controls corresponds to the

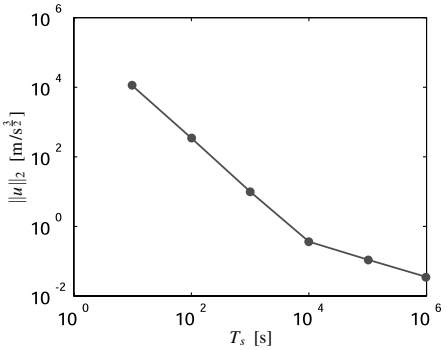

Fig. 6 Terminal time and L^2 norm of $\hat{\boldsymbol{u}}$.

Table 2 Parameters and performance indices, CSS

Parameters	Values
(a_1, a_2)	(50, 5) km
$(\bar{d}_1, \bar{d}_2)$	(0, 0) km
Performance indices	Values
$\|u\|_1$	32.590 m/s
$\|u\|_2$	3.1446×10^{-1} m/s$^{\frac{3}{2}}$
ΔV_T	49.805 m/s
T_s	37,546 s
$u_x^{\max}$	4.1752×10^{-3} m/s^2
$u_y^{\max}$	5.8159×10^{-3} m/s^2

Table 3 Parameters and performance indices, CMS

Parameters	Values
a	(50, 40, 30, 20, 10, 5) km
$\bar{d}$	(0, 0, 0, 0, 0) km
ϵ_r	(0.1, 0.2, 0.2, 0.1, 0.01)
Performance indices	Values
$\|u\|_1$	32.616 m/s
$\|u\|_2$	1.9208×10^{-1} m/s$^{\frac{3}{2}}$
ΔV_T	49.805 m/s
T_s	66,298 s
$u_x^{\max}$	1.6215×10^{-3} m/s^2
$u_y^{\max}$	2.3474×10^{-3} m/s^2

total velocity change. The L^1 norm of the feedback controller is 32.590 m/s, which is smaller than ΔV_T. Our calculations show that the L^2 norm of the feedback control decreases toward zero as Q becomes smaller relative to R, whereas the L^1 norm approaches to a positive constant. The maximum values of the inputs u_x and u_y are denoted, respectively, by $u_x^{\max}$ and $u_y^{\max}$. They are also important performance indices because they are factors that determine the specifications for the thruster. All these performance indices are given in Table 2.

The relative orbit transfer discussed above is a single-stage transfer from the initial to the final orbit, but a number of intermediate orbits may be introduced between them. The multistage transfer is then realized by the successive applications of a single-stage transfer. In the simulation four intermediate orbits with a ranging from 40 to 10 are introduced. As for the stopping rule, a suitable positive constant ϵ_r is chosen. At each stage the chaser is regarded in its final orbit if $|x|,\ |y| < \epsilon_r r_{\min}$ and $|\dot{x}|,\ |\dot{y}| < \epsilon_r v_{\min}$. One could vary ϵ_r because the chaser does not need to be strictly in each intermediate orbit. The values of the parameter ϵ_r are given in Table 3, where CMS stands for concentric and "multistage." For example $\epsilon_r = 0.1$ for the first transfer, whereas $\epsilon_r = 0.01$ for the last transfer. The trajectory of the chaser satisfying the nonlinear Hill's equations with control is depicted in Fig. 10, the control inputs in Fig. 11 and the performance indices are given in Table 3. The settling time $T_s = 66,298$ s, and the L^2 and L^1 norms of the control are 1.9208×10^{-1} m/s$^{\frac{3}{2}}$ and 32.616 m/s, respectively. Compared with the single-stage case, the settling time is longer but the L^2 norm becomes smaller. The L^1 norm, on the other hand, remains almost constant. The maximum values of acceleration become much smaller as expected and $u_x^{\max} = 1.6215 \times 10^{-3}$ m/s^2 and $u_y^{\max} = 2.3474 \times 10^{-3}$ m/s^2.

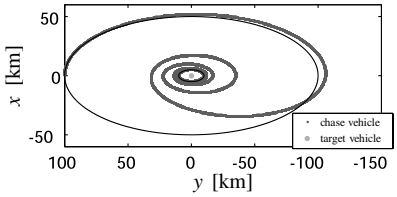

Fig. 7 Controlled trajectory of nonlinear Hill's equations, CSS.

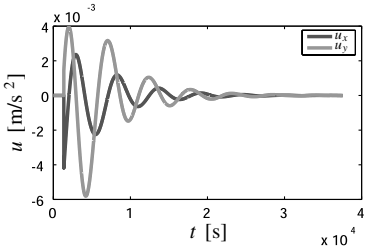

Fig. 8 Control inputs, CSS.

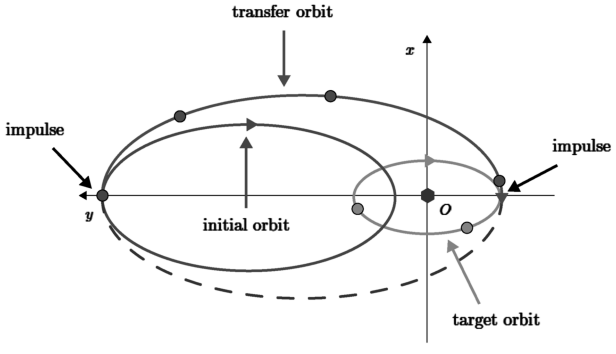

Fig. 9 Two-impulse transfer.

The transfer problem between two nonconcentric elliptic relative orbits given in Table 4 is also considered. The initial orbit is the ellipse with center $\bar{d}_1 = 25$ km and semiminor axis $\bar{a}_1 = 10$, whereas the final orbit is the ellipse with center at the origin and semiminor axis $\bar{a}_1 = 5$. The performance indices of the feedback controller are given in Table 4, where NSS stands for "nonconcentric" and "single stage." The L^1 norm of the control is 5.0564 m/s and is smaller than the total velocity change $\Delta V_T = 13.835$ m/s of the two-impulse transfer. The trajectory of the nonlinear Hill's equations with control is depicted in Fig. 12 and the control inputs in Fig. 13.

A multistage transfer between the same relative orbits is also considered. Parameters of the four intermediate orbits and the performance indices of the controller are given in Table 5, where NMS stands for "nonconcentric" and "multistage." The maximum values of acceleration $u_x^{\max}$ and $u_y^{\max}$ are 1.9329×10^{-4} m/s^2 and 5.3847×10^{-4} m/s^2, respectively, and are much smaller than those of the single-stage transfer. The controlled trajectory of the chaser is depicted in Fig. 14 and the control inputs are given in Fig. 15.

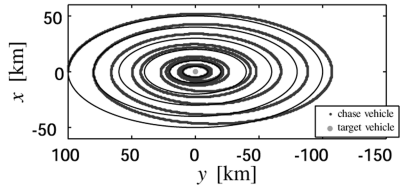

Fig. 10 Controlled trajectory of nonlinear Hill's equations, CMS.

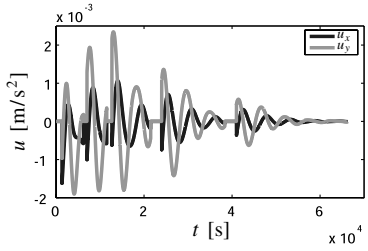

Fig. 11 Control inputs, CMS.

Table 4 Parameters and performance indices, NSS

Parameters	Values
(a_1, a_2)	(10, 5) km
$(\bar{d}_1, \bar{d}_2)$	(25, 0) km
Performance indices	Values
$\|u\|_1$	5.0564 m/s
$\|u\|_2$	6.8137×10^{-2} m/s$^{\frac{3}{2}}$
ΔV_T	13.835 m/s
T_s	25,920 s
$u_x^{\max}$	$0.826, 28 \times 10^{-3}$ m/s^2
$u_y^{\max}$	2.2899×10^{-3} m/s^2

Table 5 Parameters and performance indices, NMS

Parameters	Values
a	(10, 9, 8, 7, 6, 5) km
$\bar{d}$	(25, 20, 15, 10, 5, 0) km
ϵ_r	(0.1, 0.08, 0.05, 0.03, 0.01)
Performance indices	Values
$\|u\|_1$	4.7238 m/s
$\|u\|_2$	3.0482×10^{-2} m/s$^{\frac{3}{2}}$
ΔV_T	13.835 m/s
T_s	61,579 s
$u_x^{\max}$	1.9329×10^{-4} m/s^2
$u_y^{\max}$	5.3847×10^{-4} m/s^2

B. Relative Orbit Transfer Along an Eccentric Orbit

Assume that the target spacecraft is in an eccentric orbit. Then the relative orbits of the chaser are periodic solutions (8) of the Tschauner–Hempel equation (3). Let the initial and the final orbits be periodic solutions corresponding to the parameters K_1 and K_2 respectively. To specify the position of the target spacecraft, it is assumed that $\theta(0) = 0$ so that the target spacecraft is at perigee when $t = 0$. Let $0 \le t_0 < T$ be the initial time when the control input is introduced to the chaser. Then the initial conditions $\boldsymbol{x}_{10}$ and $\boldsymbol{x}_{20}$ of the chaser and the target are determined uniquely by (7) as functions of $\theta(t_0)$. The controlled motion of the chaser is given by

$$\dot{\boldsymbol{x}}_1 = A_1(t)\boldsymbol{x}_1 + B_1\boldsymbol{u}, \qquad \boldsymbol{x}_1(t_0) = \boldsymbol{x}_{10}$$

and the motion of the virtual vehicle by

$$\dot{\boldsymbol{x}}_2 = A_1(t)\boldsymbol{x}_2, \qquad \boldsymbol{x}_2(t_0) = \boldsymbol{x}_{20}$$

Let $\boldsymbol{x} = \boldsymbol{x}_1 - \boldsymbol{x}_2$, then

$$\dot{\boldsymbol{x}} = A_1(t)x + B_1\boldsymbol{u}, \qquad \boldsymbol{x}(t_0) = \boldsymbol{x}_0$$

where $\boldsymbol{x}_0 \equiv \boldsymbol{x}_{10} - \boldsymbol{x}_{20}$. Now consider the linear quadratic regulator problem defined by the cost function

$$J(u; \boldsymbol{x}_0) = \int_{t_0}^{\infty} [\boldsymbol{x}(t)'Q\boldsymbol{x}(t) + \boldsymbol{x}(t)'R\boldsymbol{x}(t)]\,\mathrm{d}t$$

where $Q \ge 0$, $R > 0$ and (C, A) with $C = \sqrt{Q}$ is assumed to be observable. The controllability of (A, B) ensures the existence of a positive stabilizing solution to the Riccati differential equation

$$-\dot{X} = A(t)'X + XA(t) - XBR^{-1}B'X + Q \tag{44}$$

The optimal control is given by the feedback control

$$\boldsymbol{u}^*(t) = -R^{-1}B'X(t)\boldsymbol{x}(t) \tag{45}$$

and the minimum cost by

$$J(\boldsymbol{u}^*, \boldsymbol{x}_0) = \boldsymbol{x}_0'X(t_0)\boldsymbol{x}_0 = \boldsymbol{x}[\theta(t_0)]'X(t_0)\boldsymbol{x}[\theta(t_0)] \equiv \hat{J}[\theta(t_0)]$$

Because the feedback controller (45) is stabilizing, $\boldsymbol{x}(t) \to 0$ as $t \to \infty$ and the chaser approaches the final orbit asymptotically. If $K_2 = 0$, then the final orbit becomes the origin and it corresponds to the rendezvous and docking (of the point mass systems). The minimum cost (31) is parametrized by the initial condition $\boldsymbol{x}_0$ but $\hat{J}[\theta(t_0)]$ is a function of $\theta(t_0)$. Hence $\hat{J}[\theta(t_0)]$ can be minimized with respect to $\theta(t_0)$ to obtain the best initial true anomaly.

For numerical simulations the eccentric orbit of the target spacecraft with height of perigee $h_p = 250$ km, height of apogee $h_a = 36226$ km, and eccentricity $e = 0.73074$ is considered. In this case the semimajor axis is $a_t = 24616$ km and the period of the orbit is $T = 38436$ s. These parameters are listed in Table 6. Such an orbit is often called a GTO, which is a temporary orbit to inject a satellite into the geostationary earth orbit (GEO). Note that $\theta(0) = 0$ so that the target spacecraft is at perigee when $t = 0$. The eigenvalues of the transition matrix $S_1(T, 0)$ are then calculated numerically and found $\{1, 1, 1, 1\}$, which confirms the NCVE(CVE) of the Tschauner–Hempel equation [or $(A_1(t), B_1)$].

The parameters of the initial and final orbits K_1 and K_2 are given in Table 7, where SS stands for "single stage." The maximum diameter of the initial orbit is about 50 km and that of the final orbit 10 km as shown in Fig. 16. Feedback controllers are obtained by solving (44)

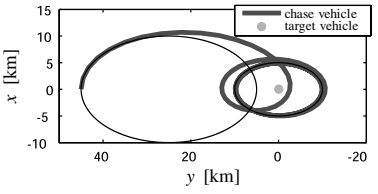

Fig. 12 Controlled trajectory of the nonlinear Hill's equations, NSS.

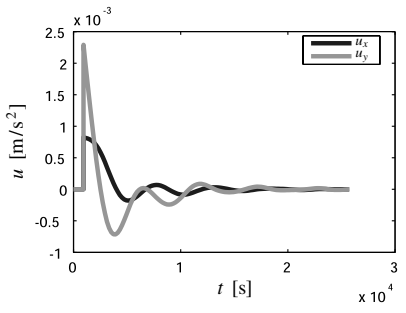

Fig. 13 Control inputs, NSS.

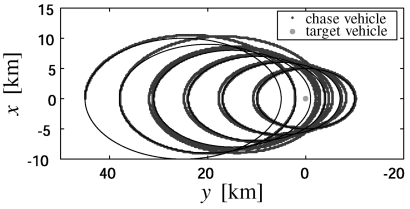

Fig. 14 Controlled trajectory of the nonlinear Hill's equations, NMS.

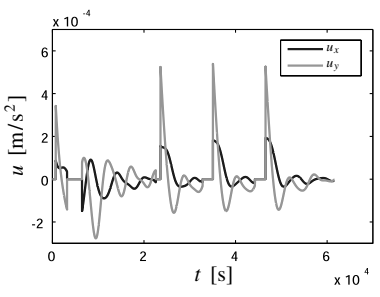

Fig. 15 Control inputs, NMS.

Table 6 Parameters of eccentric orbit

Target vehicle parameters	Values
h_p	250 km
h_a	36,226 km
e	0.730,74
a_t	24,616 km
T	38436 s

Table 7 Parameters and performance indices, SS

Parameters	Values
K_1	$[10 \quad 3 \quad 2 \quad 0]$
K_2	$[0 \quad 1 \quad 1 \quad 0]$
Performance indices	Values
$\|u\|_1$	2.5969 m/s
$\|u\|_2$	1.7864×10^{-2} m/s$^{\frac{3}{2}}$
T_s	100,341 s
$u_x^{\max}$	7.2148×10^{-4} m/s^2
$u_y^{\max}$	2.6515×10^{-3} m/s^2

numerically. To make the L^2 norm of the feedback control small, the elements $q_i (i = 1, \ldots, 4)$ of the diagonal matrix Q are taken relatively small compared with those $r_i (i = 1, 2)$ of R. Here $q_i = 1.0 \times 10^{-9}$, $i = 1, 2$, $q_i = 0$, $i = 3, 4$, and $r_i = 1.0 \times 10^7$. The linear controller is implemented to the nonlinear equations (17) and (18) with u_x and u_y, respectively. The following stopping rule is introduced. The chaser is regarded in the final orbit if $|u_x|$, $|u_y| < 1.0 \times 10^{-6}$ m/s^2. The controlled trajectory of the chaser is depicted in Fig. 16 and the control inputs in Fig. 17. The L^1 norm is 2.5969 m/s and the settling time $T_s = 100,341$ s. The maximum values of the inputs u_x and u_y are 7.2148×10^{-4} m/s^2 and 2.6515×10^{-3} m/s^2, respectively; see Table 7. The simulation results of the three-stage transfer are given in Table 8, Figs. 18 and 19, where 3S stands for "three stage." The L^1 norm remains almost constant, whereas the maximum values of acceleration become smaller in exchange for a longer settling time.

IV. Conclusions

In this paper, the relative orbit transfer problems along circular and eccentric orbits have been considered. As preliminaries, the NCVE property of Hill's equation and the Tschauner–Hempel equation have been shown. Using this property the relative orbit transfer problems are formulated as linear quadratic regulator problems and feedback controls are obtained. In the circular case the optimal cost is then minimized with respect to the initial condition. Analytical solutions are obtained when two relative orbits are concentric or when they intersect. Numerical examples show that the control strategy based on NCVE gives feedback controls with L^1 norms less than the total velocity change of the two-impulse transfer. It is also found that maximum values of control inputs decrease if the multistage transfer with intermediate orbits is employed.

In the eccentric case the feedback control is given by the periodic solution of the Riccati differential equation. Simulation results concerning an extended elliptic orbit are given and a feedback control with small L^1 norm is obtained. The proposed feedback controller could be applied to the transfer problem between any initial and final trajectories that are not necessarily periodic.

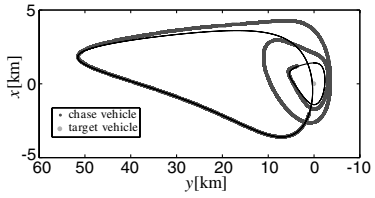

Fig. 16 Controlled trajectory of the nonlinear Tschauner–Hempel equation, SS.

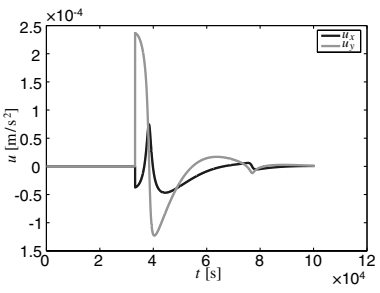

Fig. 17 Control inputs, SS.

Table 8 Parameters and performance indices, 3S

Parameters	Values
K_1	$[10 \quad 3 \quad 2 \quad 0]$
K_2	$[5 \quad 2 \quad 1 \quad 0]$
K_3	$[0 \quad 1 \quad 2 \quad 0]$
K_4	$[0 \quad 1 \quad 1 \quad 0]$
Performance indices	Values
$\|u\|_1$	2.7873 m/s
$\|u\|_2$	1.2718×10^{-2} m/s$^{\frac{3}{2}}$
T_s	243795 s
$u_x^{\max}$	1.4748×10^{-4} m/s^2
$u_y^{\max}$	1.4756×10^{-3} m/s^2

Appendix: Necessary and Sufficient Conditions for Null Controllability with Vanishing Energy

I. Null Controllability with Vanishing Energy

In this Appendix the notion of NCVE is introduced and its useful necessary and sufficient conditions are given.

Consider

$$\dot{x} = Ax + Bu, \qquad x(0) = x_0 \tag{A1}$$

where $x \in \boldsymbol{R}^n$, $u \in \boldsymbol{R}^m$, $y \in \boldsymbol{R}^p$, and u is a locally square integrable function. The solution is denoted by $x(t; x_0, u)$. The following definitions are introduced in [23].

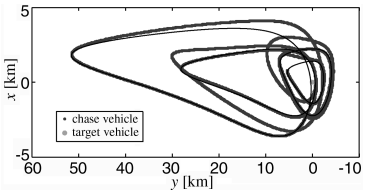

Fig. 18 Controlled trajectory of the nonlinear Tschauner–Hempel equation, 3S.

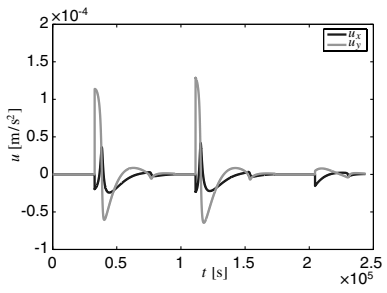

Fig. 19 Control inputs, 3S.

Definition A1. 1) The system (A1) is said to be null controllable with vanishing energy, if for any x_0, there exists a sequence of pairs $\{T_N, u_N\}$, $0 < T_N \to \infty$ as $N \to \infty$, $u_N \in L^2(0, T_N; \boldsymbol{R}^m)$ such that

$$x(T_N; x_0, u_N) = 0 \quad \text{and} \quad \lim_{N\to\infty} \int_0^{T_N} |u_N(t)|^2 \, \mathrm{d}t = 0$$

In this case (A, B) is called NCVE. 2) The system (A1) is said to be controllable with vanishing energy, if for any pair $\{x_0, x_1\}$, there exists a sequence of pairs $\{T_N, u_N\}$, $0 < T_N \to \infty$ as $N \to \infty$, $u_N \in L^2(0, T_N; \boldsymbol{R}^m)$ such that

$$x(T_N; x_0, u_N) = x_1 \quad \text{and} \quad \lim_{N\to\infty} \int_0^{T_N} |u_N(t)|^2 dt = 0$$

In this case (A, B) is called CVE.

Statement 1 implies that any initial state can be steered to the origin with a control of arbitrarily little energy. And the energy here is understood in the sense of L^2 norm. The main results of [23] in finite dimensions yield the following theorems.

Theorem A1. 1) (A, B) is NCVE if and only if it is controllable and $X = 0$ is the unique solution to the algebraic Riccati equation

$$A'X + XA - XBB'X = 0 \tag{A2}$$

in the class of nonnegative matrices. 2) (A, B) is NCVE if and only if it is controllable and $Re\lambda \leq 0$ for any $\lambda \in \sigma(A)$ where $\sigma(A)$ is the set of all eigenvalues of A.

Theorem A1 was originally proved in Hilbert space in [23] and the part 1 was then extended to Banach space in [25].

Theorem A2. (A, B) is CVE if and only if it is controllable, and $Re\lambda = 0$ for any $\lambda \in \sigma(A)$.

Remark A1. The ARE (A2) can be replaced by

$$A'X + XA - XBR^{-1}B'X = 0$$

for any positive definite matrix $R > 0$. In fact (A, B) is NCVE if and only if $(A, BR^{-\frac{1}{2}})$ is NCVE.

A useful consequence of NCVE on the linear quadratic regulator is in order. Consider the quadratic cost for (A1)

$$J(u; x_0) = \int_0^\infty [|Cx(t)|^2 + u'(t)Ru(t)] \, \mathrm{d}t$$

where R is positive definite and $|\cdot|$ denotes the Euclidean norm. The following results are known [21,22]. Suppose (A, B) is stabilizable and (C, A) detectable. Then there exists a unique nonnegative solution X to the ARE

$$A'X + XA - XBR^{-1}B'X + C'C = 0$$

such that $A - BR^{-1}B'X$ is exponentially stable. The optimal control minimizing $J(u; x_0)$ is given by the feedback control $u^* = -R^{-1}B'Xx$ and $J(u^*; x_0) = x_0'Xx_0$. If (C, A) is observable, the solution X in part 1 is positive definite. If (A, B) is NCVE, then $X \to 0$ and hence $J(u^*; x_0) \to 0$ as $C'C \to 0$. Thus the initial state x_0 can be steered asymptotically to the origin with arbitrarily little control effort. In applications the L_2 norm of the feedback control $u^* = -R^{-1}B'Xx$ can be made arbitrarily small by choosing $C'C$ small.

II. Null Controllability with Vanishing Energy for Periodic Systems

Consider the system

$$\dot{x} = A(t)x + B(t)u, \qquad x(t_0) = x_0$$

where $A(t)$ and $B(t)$ are T-periodic continuous functions.

$[A(t), B(t)]$ is said to be controllable on $[t_0, \tau]$ if for any x_0 and x_1, there exists a control such that $x(\tau; x_0, u) = x_1$. $[A(t), B(t)]$ is controllable on $[t_0, \tau]$ if and only if

$$\int_{t_0}^{\tau} S(\tau, r)B(r)B'(r)S'(\tau, r) \, \mathrm{d}r > 0$$

where $S(t, s)$ is the transition matrix generated by $A(t)$. If $[A(t), B(t)]$ is controllable on $[t_0, \tau]$, then it is controllable on any interval $[t_0, \tau_1]$, $\tau_1 \geq \tau$. NCVE and CVE of $[A(t), B(t)]$ on $[t_0, \infty)$ are defined as in Definition A1.

Theorems A1 and A2 are extended to periodic systems as follows [26–28].

Theorem A3. 1) $[A(t), B(t)]$ is NCVE on $[t_0, \infty)$ if and only if $[A(t), B(t)]$ is controllable on some interval $[t_0, \tau]$, and $X(t) = 0$ is the unique solution to the differential Riccati equation

$$-\dot{X} = A'X + XA - XBB'X$$

in the class of T-periodic nonnegative matrices. 2) $[A(t), B(t)]$ is NCVE on $[t_0, \infty)$ if and only if $[A(t), B(t)]$ is controllable on some interval $[t_0, \tau]$, and $|\lambda| \leq 1$ for any $\lambda \in \sigma[S(T, 0)]$.

The second condition is obtained by considering the discrete-time system for $x(kT)$.

Theorem A4. $[A(t), B(t)]$ is CVE on $[t_0, \infty)$ if and only if $[A(t), B(t)]$ is controllable on some interval $[t_0, \tau]$, and $|\lambda| = 1$ for any $\lambda \in \sigma[S(T, 0)]$.

Consider the quadratic cost

$$J(u; x_0) = \int_{t_0}^\infty [|C(t)x(t)|^2 + u'(t)R(t)u(t)] \, \mathrm{d}t$$

where $C(t)$ and $R(t) > 0$ are T periodic. As in the time-invariant case, the following results are known [29]. Suppose $[A(t), B(t)]$ is stabilizable and $[C(t), A(t)]$ detectable. Then there exists a unique nonnegative T-periodic solution X to the Riccati differential equation

$$-\dot{X} = A'X + XA - XBB'X + C'C$$

such that $A(t) - B(t)R^{-1}(t)B'(t)X(t)$ is asymptotically stable. The optimal control minimizing $J(u; x_0)$ is given by the feedback control $u^* = -R^{-1}(t)B'(t)X(t)x$ and $J(u^*; x_0) = x_0'X(t_0)x_0$. If $[C(t), A(t)]$ is observable on some interval $[t_0, \tau]$, then $X(t) > 0$. Again choosing $C'C$ small and using the feedback control $u^* = -R^{-1}(t)B'(t)X(t)x$, the initial state can be steered to the origin with arbitrarily little control effort. Theorem A3 is used in Sec. III to design feedback laws for relative orbit transfer problems.

Acknowledgments

The authors would like to thank K. Tsuchiya of Kyoto University for introducing them to the orbital rendezvous problem and for helpful comments on this work, and K. Masuda of Nagoya Guidance and Propulsion Systems Works, Mitsubishi Heavy Industries, Ltd., and S. Kimura of National Institute of Information and Communication Technology for introducing them to the SmartSat-1 project and for helpful discussions on this work. The authors also would like to thank the reviewers for valuable comments and suggestions on the paper.

References

[1] Prussing, J. A., and Conway, B. A., *Orbital Mechanics*, Oxford University Press, New York, 1993, pp. 139–152.

[2] Vallado, D. A., *Fundamentals of Astrodynamics and Applications*, 2nd ed., Kluwer Academic, Boston, 2001, pp. 374–399.

[3] Wie, B., *Space Vehicle Dynamics and Control*, AIAA, New York, 1998, pp. 282–285.

[4] Clohessy, W. H., and Wiltshire, R. S., "Terminal Guidance System for Satellite Rendezvous," *Journal of Aerospace Science*, Vol. 27, No. 5, 1960, pp. 653–658.

[5] Prussing, J. E., "Optimal Two- and Three-Impulse Fixed-Time Rendezvous in the Vicinity of a Circular Orbit," *AIAA Journal*, Vol. 8, No. 7, 1970, pp. 1221–1228.

[6] Jezewsky, D. J., and Donaldson, J. D., "Analytic Approach to Optimal Rendezvous Using Clohessy–Wiltshire Equations," *Journal of the Astronautical Sciences*, Vol. 27, No. 3, 1979, pp. 293–310.

[7] Carter, T. E., "State Transition Matrices for Terminal Rendezvous Studies: Brief Survey and New Example," *Journal of Guidance, Control, and Dynamics*, Vol. 21, No. 1, 1998, pp. 148–155.

[8] Singla, P., Subbarao, K., and Junkins, J. L., "Adaptive Output Feedback Control for Spacecraft Rendezvous and Docking Under Measurement Uncertainty," *Journal of Guidance, Control, and Dynamics*, Vol. 29, No. 4, 2006, pp. 892–902.

[9] Vassar, R. H., and Sherwood, R. B., "Formationkeeping for a Pair of Satellites in a Circular Orbit," *Journal of Guidance, Control, and Dynamics*, Vol. 8, No. 2, 1985, pp. 235–242.

[10] Leonard, C. L., Hollister, W. M., and Bergmann, E. V., "Orbital Formationkeeping with Differential Drag," *Journal of Guidance, Control, and Dynamics*, Vol. 12, No. 1, 1989, pp. 108–113.

[11] Redding, D. C., Adams, N., and Kubiak, E. T., "Linear-Quadratic Stationkeeping for the STS Orbiter," *Journal of Guidance, Control, and Dynamics*, Vol. 12, No. 2, 1989, pp. 248–255.

[12] Kapila, V., Sparks, A. G., Buffington, J. M., and Yan, Q., "Spacecraft Formation Flying: Dynamics and Control," *Journal of Guidance, Control, and Dynamics*, Vol. 23, No. 3, 2000, pp. 561–564.

[13] Kang, W., Sparks, A., and Banda, S., "Coordinate Control of Multisatellite Systems," *Journal of Guidance, Control, and Dynamics*, Vol. 24, No. 2, 2001, pp. 360–368.

[14] Vaddi, S. S., Alfriend, K. T., Vadali, S. R., and Sengupta, P., "Formation Establishment and Reconfiguration Using Impulsive Control," *Journal of Guidance, Control, and Dynamics*, Vol. 28, No. 2, 2005, pp. 262–268.

[15] de Queiroz, M. S., Kapila, V., and Yan, Q., "Adaptive Nonlinear Control of Multiple Spacecraft Formation Flying," *Journal of Guidance, Control, and Dynamics*, Vol. 23, No. 3, 2000, pp. 385–390.

[16] Yeh, H. H., Nelson, E., and Sparks, A., "Nonlinear Tracking Control for Satellite Formations," *Journal of Guidance, Control, and Dynamics*, Vol. 25, No. 2, 2002, pp. 376–386.

[17] Palmer, P., "Optimal Relocation of Satellites Flying in Near-Circular-Orbit Formations," *Journal of Guidance, Control, and Dynamics*, Vol. 29, No. 3, 2006, pp. 519–526.

[18] Carter, T. E., and Brient, J., "Linearized Impulsive Rendezvous Problem," *Journal of Optimization Theory and Applications*, Vol. 86, No. 3, 1995, pp. 553–584.

[19] Yamanaka, K., and Ankersen, F., "New State Transition Matrix for Relative Motion on an Arbitrary Elliptical Orbit," *Journal of Guidance, Control, and Dynamics*, Vol. 25, No. 1, 2002, pp. 60–66.

[20] Inalhan, G., Tillerson, M., and How, J. P., "Relative Dynamics and Control of Spacecraft Formations in Eccentric Orbits," *Journal of Guidance, Control, and Dynamics*, Vol. 25, No. 1, 2002, pp. 48–59.

[21] Callier, F. M., and Desoer, C. A., *Linear System Theory*, Springer–Verlag, Berlin, 1991, pp. 330–355.

[22] Wonham, W. M., *Linear Multivariable Control: A Geometric Approach*, 3rd ed., Springer–Verlag, New York, 1985, pp. 276–289.

[23] Priola, E., and Zabczyk, J., "Null Controllability with Vanishing Energy," *SIAM Journal on Control and Optimization*, Vol. 42, No. 3, 2003, pp. 1013–1032.

[24] Ivanov, S., "Control Norms for Large Control Times," *ESAIM: Control Optimisation, and Calculus of Variations*, Vol. 4, 1999, pp. 405–418.

[25] Van Neerven, J. M. A. M., "Null Controllability and the Algebraic Riccati Equation in Banach Spaces," *SIAM Journal on Control and Optimization*, Vol. 43, No. 4, 2005, pp. 1313–1327.

[26] Ichikawa, A., "Null Controllability with Vanishing Energy for Infinite Dimensional Periodic Systems," *Proceedings of the Seventeenth International Symposium on Mathematical Theory of Networks and Systems*, 2006, pp. 638–642.

[27] Ichikawa, A., "Null Controllability with Vanishing Energy for Discrete-Time Systems," Department of Aeronautics and Astronautics, Kyoto University, Rept. Control-1, Kyoto, Japan, Aug. 2006.

[28] Ichikawa, A., "Null Controllability with Vanishing Energy for Discrete-Time Systems in Hilbert Space," *SIAM Journal on Control and Optimization* (to be published).

[29] Ichikawa, A., and Katayama, H., *Linear Time Varying Systems and Sampled-Data Systems*, Springer–Verlag, London, 2001, pp. 19–27.